



HAL
open science

Internal wave generation by turbulent wakes

Bruno Voisin

► **To cite this version:**

Bruno Voisin. Internal wave generation by turbulent wakes. Meeting-Workshop on Mixing in Geophysical Flows, Effects of Body Forces in Turbulent Flows, Dec 1992, Barcelona, Spain. pp.291-301. hal-01944149

HAL Id: hal-01944149

<https://hal.science/hal-01944149>

Submitted on 4 Dec 2018

HAL is a multi-disciplinary open access archive for the deposit and dissemination of scientific research documents, whether they are published or not. The documents may come from teaching and research institutions in France or abroad, or from public or private research centers.

L'archive ouverte pluridisciplinaire **HAL**, est destinée au dépôt et à la diffusion de documents scientifiques de niveau recherche, publiés ou non, émanant des établissements d'enseignement et de recherche français ou étrangers, des laboratoires publics ou privés.

INTERNAL WAVE GENERATION BY TURBULENT WAKES

BRUNO VOISIN

*Laboratoire des Écoulements Géophysiques et Industriels,
Institut de Mécanique de Grenoble, CNRS – UJF – INPG,
BP 53X, 38041 Grenoble Cedex, France*

At high Froude and Reynolds numbers, lee waves generated by a body moving horizontally in a stratified fluid give way to ‘random’ internal waves generated by the turbulent wake. This paper considers the second type of waves, whose presence is attributed to the collapse of vortex loops or turbulent bursts, associated with the coherent vortex structures of the wake. A simple analytical model of the collapse is given, leading to two distinct analyses of the waves. At moderate cross-stream distances the individual effect of each loop or burst is observed; waves have the same structure as for an isolated impulsive point source. At large cross-stream distances the collective effect of the loops or bursts is observed; waves reduce to those generated by a source of mass moving with the body, and emitting fluid at the frequency of vortex shedding and at some of its harmonics. Here, only the fundamental frequency is taken into account, in which case the waves decompose into several systems and are confined within conical caustics. All of this agrees with available experimental results. More attention is finally paid to the shape of surfaces of constant phase.

1. Introduction

Stratified flows of geophysical interest are often characterised by complicated combination of, and strong interaction between, turbulence and internal gravity waves. They are governed by two dimensionless parameters, the Reynolds number Re representing the ratio of inertial forces to viscous forces, and the internal Froude number Fr representing the ratio of inertial forces to buoyancy forces. For instance, for sufficiently low Fr , homogeneous stratified turbulence decreases more rapidly than its unstratified counterpart, as a result of both the buoyant collapse of the large-scale eddies and the subsequent radiation of internal waves (see, e.g., [1]). Similarly, for sufficiently high Re , lee waves, i.e., internal waves generated by horizontal stratified flow past a fixed obstacle or by horizontal motion of a body in a stratified fluid at rest, are superseded by ‘random’ waves generated by the turbulent wake of this obstacle or body. This paper considers the second aspect, namely internal wave radiation by a three-dimensional turbulent wake.

The first mention of this phenomenon dates back to Lin & Pao [2], who noticed that “[when] turbulence has decayed appreciably, random internal waves appeared near the wake boundary”. The existence of these waves was then confirmed, and its origin clarified, by experiments carried out by Gilreath & Brandt [3] for a self-propelled slender spheroid and by Hopfinger *et al.* [4] and Bonneton *et al.* [5] for a towed sphere. In fact, the internal wave field accompanying a horizontally moving body comprises several distinct components: deterministic lee waves generated by the body itself; deterministic waves observed only in the self-propelled case, and generated by the collapse of the wake due to initial mixing and by the propeller swirl; random internal waves generated by the turbulent wake, at Reynolds numbers $Re = 2aU/\nu$ such that this wake is turbulent. Here ν is the kinematic viscosity, N the buoyancy frequency, a the transverse radius

of the body and U its velocity. Of all those components only the latter is stationary relative to the fluid, the others being stationary relative to the body. At small Froude numbers $Fr = U/Na$, deterministic waves are dominant and the wavelength is roughly equal to $2\pi U/N$; as Fr increases they are progressively blurred by the smaller random waves, until eventually, for $Fr \gtrsim 4.5$, these waves become dominant.

Our aim here is not to discuss experimental results any further, neither to present theories for the calculation of the deterministic waves. For such theories the reader is referred to the author's Ph.D. thesis [6] and to, among others, the papers by Miles [7], Makarov & Chashechkin [8], Janowitz [9] and Umeki & Kambe [10] for lee waves, and by Hartman & Lewis [11], Meng & Rottman [12] and Gorodtsov [13, 14] for deterministic wake-generated waves. In the following we shall, rather, present preliminary theoretical investigations of random waves, by discussing in §2 the modelling of the turbulent wake as a source of internal waves, and by analysing in §§3 and 4 the waves generated by two simplified versions of the model.

2. Wake model

There is increasing evidence (Bonneton & Chomaz [15]; Chomaz *et al.* [16]) that the formation of homogeneous turbulent wakes results from the combination of two modes of instability of the recirculation zone immediately behind moving bodies: Kelvin-Helmholtz instability of the shear layer at the boundary of this zone, and spiral instability associated with the rotation of the separation point. For a sphere the two modes are locked and of identical Strouhal numbers for $Re \lesssim 800$, while for $Re \gtrsim 800$ they are unlocked; then the Kelvin-Helmholtz mode is of smaller wavelength (larger shedding frequency f) and Strouhal number $St = 2af/U$ varying as $Re^{1/2}$, while the spiral mode is of larger wavelength (smaller shedding frequency f) and Strouhal number $St \approx 0.2$ roughly independent of Re .

When stratification comes into play a wide variety of flow configurations is encountered. For $Fr \gtrsim 4.5$, however, and Re such that the flow is fully turbulent, stratification becomes so weak that the near wake of a sphere develops initially as in unstratified fluid, before being affected by gravity at the dimensionless time $Nt_c \approx 3$; then the connected vortex loops forming the spiral instability collapse [16]. From the observation that ‘random’ internal waves are noticeable only in precisely that Reynolds and Froude numbers range, Hopfinger *et al.* [4] and Bonneton *et al.* [5] have identified the origin of the random waves as the collapse of each vortex loop. The same phenomenon has been reported by Sysoeva & Chashechkin [17, 18] at lower Reynolds numbers when each vortex loop is well separated from the others, and is probably responsible for the random-like wake-generated internal waves visualised by Boyer *et al.* [19] behind a cylinder and by Lin *et al.* [20] behind a sphere.

This, to be true, applies only to towed bodies. For self-propelled bodies the wake is momentumless, and may be viewed as the combination of a pure wake (with momentum defect) and a pure jet (with momentum excess). The two vortex structures associated with these configurations interact, as a result of which intermittent ‘bursts’ of turbulence are observed instead a large-scale well-organised vortical structure, with mean burst spacing roughly equal to the transverse diameter of the body, in other terms with effective Strouhal number $St \approx 1$ (see, in two dimensions, Cimbalá & Park [21] and in three dimensions Higuchi & Kubota [22]). When the fluid is stratified, the bursts collapse following their violent rise in the near wake and, as in the towed case, generate ‘random’ internal waves (Gilreath & Brandt [3]).

Now, the pioneering experiments of Wu [23] have shown that the buoyant collapse of any density or velocity perturbation of a stratified fluid acts as an impulsive source of internal waves. Thus, as regards these waves, a turbulent wake is amenable to a discrete distribution of impulsive sources and sinks, periodically spaced in both space and time, and each of which represents the collapse of a vortex loop or turbulent burst. Neglecting entrainment velocity, we can write the

temporal period of this distribution as $1/f = 2\pi/\omega_0$ and its spatial period as $U/f = 2a/St = 2\pi U/\omega_0$, where $\omega_0 = 2\pi f$ is the angular frequency of vortex shedding or burst release. Neglecting, moreover, the quadrupolar nature of each collapsing event (Miles [7]), we replace it by a monopole, and choose the sign of this monopole to be alternately positive and negative from one event to the next, to take phenomenologically into account the symmetry of the wake. In this way the turbulent wake reduces to the mass source

$$m(\mathbf{r}, t) = m_0 \sum_{n=-\infty}^{+\infty} (-1)^n \delta\left(x + n\frac{\pi U}{\omega_0}\right) \delta(y) \delta(z) \delta\left(t - n\frac{\pi}{\omega_0}\right), \quad (2.1)$$

alternately releasing and absorbing a volume m_0 of fluid (figure 1), and related to the fluid velocity $\mathbf{v}(\mathbf{r}, t)$ by $\nabla \cdot \mathbf{v} = m$. Here a fixed system of coordinates (x, y, z) is used, with the x -axis horizontal and directed opposite to the motion of the body, the z -axis directed vertically upwards, and the y -axis horizontal and transverse. The choice of the time and space origins is arbitrary, and depends on the time of start of vortex shedding or burst release.

The source (2.1) is of course only a very crude approximation to the real process of emission of the waves; it will, nevertheless, be shown to provide useful quantitative information on them. One point, however, is worth being discussed into greater detail before proceeding any further: the randomness of the waves. First, turbulence-generated internal waves are, at any particular place, random from one realisation to another of exactly the same experiment [3]; this is attributable in (2.1) to the random character of the time of start of vortex shedding or burst release. Second, those waves are, for any particular experimental realisation, random from one place to another [4], [5] (i.e., they have poor spatial coherence); this is attributable to the fact that the collapsing spiral structure modelled by (2.1) is immersed in turbulence, which induces a random modulation of the duration π/ω_0 and distance $\pi U/\omega_0$ between successive impulses.

In spite of all those approximations, the assembly (2.1) of time- and space-lagged impulsive point sources is still too complicated to be treated in this form. Instead, we rewrite it as

$$m(\mathbf{r}, t) = m_0 \delta(x + Ut) \delta(y) \delta(z) \sum_{n=-\infty}^{+\infty} (-1)^n \delta\left(t - n\frac{\pi}{\omega_0}\right), \quad (2.2)$$

namely as a point source moving horizontally and uniformly at velocity U while emitting impulses at time intervals π/ω_0 . Applying then Poisson sum formula [24, pp. 466–467], we deduce

$$m(\mathbf{r}, t) = \frac{\omega_0 m_0}{\pi} \delta(x + Ut) \delta(y) \delta(z) \sum_{n=-\infty}^{+\infty} \exp[i(2n + 1)\omega_0 t], \quad (2.3)$$

namely a third representation of the turbulent wake as a point source moving horizontally and uniformly at velocity U while oscillating at the frequency ω_0 and at all its odd harmonics.

Two simplified models arise then naturally, whose relevance depends on the distance to the wake. The first model is valid at small distances, where impulsive waves associated with each collapsing loop or burst have not yet had time to interfere. Then it is legitimate to consider the individual effect of each of these sources separately, and accordingly to retain only one term in the sum (2.1). On the other hand, at large distances the interference pattern is well-developed, so that only the collective effect of all the sources is observed, in the form of the generation of the frequency ω_0 and of its harmonics. In practice, as a consequence of the collapsing events being neither perfectly localised in time nor in space, the fundamental frequency is dominant. It is then legitimate to retain only this frequency in (2.3), which reduces but to the model proposed by Gilreath & Brandt [3], shown dashed in figure 1.

In what follows we shall examine individually and collectively generated waves successively, and in particular compare their characteristics with the few experimental results available.

3. Individual wave generation

According to (2.1), each collapse acts as the impulsive point mass source

$$m(\mathbf{r}, t) = m_0 \delta(\mathbf{r}) \delta(t). \quad (3.1)$$

This is just the source associated with the Green's function $G(\mathbf{r}, t)$ of internal waves, about which a synthesis has recently been proposed by Voisin [25]. In particular, the wavy nature of $G(\mathbf{r}, t)$ becomes explicit in the large-time limit $Nt \gg 1$, in which case

$$G(\mathbf{r}, t) \sim -\frac{m_0}{(2\pi)^{\frac{3}{2}} N r \sin \theta} \left[\frac{\cos(Nt |\cos \theta| - \pi/4)}{(Nt |\cos \theta|)^{\frac{1}{2}}} + \frac{\sin(Nt - \pi/4)}{(Nt)^{\frac{1}{2}}} \right], \quad (3.2)$$

as first obtained by Dickinson [26], rederived later by Sekerzh-Zen'kovich [27] and investigated into greater detail by Zavol'skii & Zaitsev [28]; a spherical system of coordinates (r, θ, φ) has been introduced, with θ the angle to the z -axis (figure 2).

Thus, internal waves comprise two terms. The first of them, called *gravity waves*, is made of propagating waves of frequency $\omega = N |\cos \theta|$ conformable to the group velocity theory, phase $\Phi = Nt |\cos \theta|$ constant on cones of vertical axis (figure 3), and wavelength

$$\lambda = \frac{2\pi r}{Nt \sin \theta} \quad (3.3)$$

decreasing linearly with time. The second term, called *buoyancy oscillations*, corresponds to non-propagating oscillations at the resonance frequency N of the medium. The relative importance of these terms is set up by their amplitudes, whose study requires the replacement of the Green's function G (a generalised velocity potential) by a physically more meaningful quantity, such as the vertical displacement $\zeta = \partial^2 G / \partial z \partial t$. In the large-time limit $Nt \gg 1$, this displacement reduces to

$$\zeta(\mathbf{r}, t) \sim \frac{m_0}{(2\pi)^{\frac{3}{2}} r^2} \operatorname{sgn} z \left[\sin \theta (Nt |\cos \theta|)^{\frac{1}{2}} \cos\left(Nt |\cos \theta| - \frac{\pi}{4}\right) - \frac{\cos \theta}{|\sin \theta|^3} \frac{\sin(Nt - \pi/4)}{(Nt)^{\frac{3}{2}}} \right], \quad (3.4)$$

indicating that the amplitude of gravity waves is maximum in the direction

$$\theta_m = \arctan \sqrt{2} \approx 55^\circ \quad (3.5)$$

where $\sin \theta |\cos \theta|^{1/2}$ is maximum, and that these waves, which increase with time as $t^{1/2}$, are dominant compared with the decreasing (as $t^{-3/2}$) buoyancy oscillations, at least before the wavelength has become so small that gravity waves are blurred by destructive interference owing to the finite extent of any real source. All of those characteristics are confirmed by the experiments of Stevenson [29] and McLaren *et al.* [30] for the impulsive motion of cylinders and spheres.

Similar experiments were carried out by Bonneton *et al.* [5] for internal waves generated by the turbulent wake of a sphere, at moderate distances from this wake. Various visualisation methods have shown that surfaces of constant phase are concentric circles in any horizontal plane and fan-like lines in the vertical plane containing the path of the sphere; this is consistent with a three-dimensional conical shape. Combination of probe measurements and flow visualisations has, moreover, confirmed the decrease of the wavelength as t^{-1} and the existence of a direction of maximum wave amplitude. Note, however, that the exact value of the angle θ_m of this direction to the vertical depends on the form of the amplitude, which in turn depends on the quantity investigated (i.e., on the visualisation method used) and on the exact multipolar nature of the source (assumed here to be a monopole).

4. Collective wave generation

We turn now to the analysis of collective wave generation, which, according to (2.3), we ascribe to the uniformly moving source of oscillatory strength

$$m(\mathbf{r}, t) = \frac{\omega_0 m_0}{\pi} e^{i\omega_0 t} \delta(x_1) \delta(y) \delta(z). \quad (4.1)$$

Hereafter moving systems of cartesian coordinates ($x_1 = x + Ut, y, z$) and spherical coordinates (r_1, θ_1, φ_1) will be used, with θ_1 the angle to the x_1 -axis and φ_1 the angle to the plane $z = 0$ (figure 4). This problem has been studied in two dimensions by Stevenson & Thomas [31], and in three dimensions by Redekopp [32], Rehm & Radt [33] and Peat & Stevenson [34], emphasis being placed on the shape of surfaces of constant phase. We, rather, adopt the approach exposed in Voisin [35], in which the amplitude and the phase of the waves are obtained jointly.

The clue here is the introduction of the reduced Doppler frequency

$$\xi = \frac{\omega}{N}, \quad (4.2)$$

such that $|\xi| < |\sin \varphi_1|$, and of the reduced source frequency

$$\Upsilon = \frac{\omega_0}{N} = \pi FrSt, \quad (4.3)$$

which, in the Froude and Strouhal numbers range where random internal waves are observed, is always larger than 1. Waves are stationary relative to the source. They are expressed in terms of r_1, θ_1, φ_1 and of the additional variable ξ which, for given θ_1 and φ_1 , satisfies the equation

$$\tan \theta_1 = \frac{\xi^2 (\sin^2 \varphi_1 - \xi^2)^{\frac{1}{2}}}{\Upsilon \sin^2 \varphi_1 - \xi^3}, \quad (4.4)$$

solved graphically in figure 5. Two systems of waves are present, called *sum waves* ($-|\sin \varphi_1| < \xi < 0$) and *difference waves* ($0 < \xi < |\sin \varphi_1|$), each of which is itself separated into *transverse waves* and *divergent waves* (this applies only to the case $\Upsilon > 1$).

All waves are found downstream of the source and are confined within caustics, which correspond to the maxima of the curve in figure 5 and are given by the equation, represented in figure 6,

$$\theta_1 = \Theta_{\pm} = \arctan \left[\frac{\Xi_{\pm}^2}{3\Upsilon (\sin^2 \varphi_1 - \Xi_{\pm}^2)^{\frac{1}{2}}} \right], \quad (4.5a)$$

$$\xi = \Xi_{\pm} = \Upsilon \left\{ 1 - 2 \cos \left[\frac{1}{3} \arccos \left(1 - \frac{\sin^2 \varphi_1}{\Upsilon^2} \right) \pm \frac{\pi}{3} \right] \right\}, \quad (4.5b)$$

where the subscript $+$ ($-$) stands for sum (difference) waves, respectively. Those caustics are represented in figure 7 for $\Upsilon = 1.2$, and are pairs of cones symmetric with respect to the plane $z = 0$. As Υ increases they differ less and less (by a slight stretching along the vertical for sum waves and by a slight shrinking for difference waves) from pairs of circular cones of apex at the source and axis in the plane $y = 0$. For $\Upsilon \gg 1$ they tend asymptotically to these cones, according to

$$\Xi_{\pm} \sim \pm \left(\frac{2}{3} \right)^{\frac{1}{2}} |\sin \varphi_1|, \quad \Theta_{\pm} \sim \frac{2}{3^{\frac{3}{2}}} \frac{|\sin \varphi_1|}{\Upsilon}, \quad (4.6)$$

as shown in figure 6. Transverse waves and divergent waves merge on the caustics, and correspond to $0 < |\xi_{\pm}| < |\Xi_{\pm}|$ and $|\Xi_{\pm}| < |\xi_{\pm}| < |\sin \varphi_1|$, respectively.

Internal waves can, as before, be expressed in terms of a generalised velocity potential $\psi(\mathbf{r}, t)$, to which the vertical displacement is related by $\zeta = \partial^2 \psi / \partial z \partial t$. In the far field $Nr_1/U \gg 1$, sum waves and divergence waves become, respectively,

$$\psi_{\pm}(\mathbf{r}, t) \sim -H(\Theta_{\pm} - \theta_1) \frac{\omega_0 m_0}{4\pi^2 N^2 x_1} \exp\left\{i\left[\Phi_{\pm} \mp \frac{\pi}{2} H(|\xi_{\pm}| - |\Xi_{\pm}|)\right]\right\} \\ \times \frac{\Upsilon \sin^2 \varphi_1 - \xi_{\pm}^3}{|\xi_{\pm} \sin \varphi_1| |(1 - \xi_{\pm}^2)(\Upsilon - \xi_{\pm})(\xi_{\pm}^3 - 3\Upsilon \xi_{\pm}^2 + 2\Upsilon \sin^2 \varphi_1)|^{\frac{1}{2}}}, \quad (4.7)$$

where H denotes the Heaviside step function and the phase Φ_{\pm} has the two equivalent forms

$$\Phi_{\pm} = \omega_0 t - \frac{N}{U} x_1 \frac{(\Upsilon - \xi_{\pm})^2 \sin^2 \varphi_1}{\Upsilon \sin^2 \varphi_1 - \xi_{\pm}^3} = \omega_0 t - \frac{N}{U} r_{\perp} \frac{(\Upsilon - \xi_{\pm})^2 \sin^2 \varphi_1}{\xi_{\pm}^2 (\sin^2 \varphi_1 - \xi_{\pm}^2)^{\frac{1}{2}}}, \quad (4.8)$$

where $r_{\perp} = (y^2 + z^2)^{1/2}$ represents transverse distances. As usual, this leading-order expansion breaks down in the vicinity of caustics.

We shall limit our investigations here to the shape of the surfaces of constant phase, defined as surfaces of constant $\Phi_{\star} = \omega_0 t - \Phi_{\pm}$. From (4.8) we deduce the parametric equation, expressed in terms of the reduced coordinates $\mathbf{r}_{\star} = (N\mathbf{r}_1)/(U\Phi_{\star})$,

$$x_{\star} = \frac{\Upsilon \sin^2 \varphi_1 - \xi^3}{(\Upsilon - \xi)^2 \sin^2 \varphi_1}, \quad r_{\perp \star} = \frac{\xi^2 (\sin^2 \varphi_1 - \xi^2)^{\frac{1}{2}}}{(\Upsilon - \xi)^2 \sin^2 \varphi_1}. \quad (4.9)$$

A perspective view of those surfaces for $\Upsilon = 1.2$ is given in figure 8, and is accompanied in figure 9 by a more quantitative representation in terms of intersections by vertical or horizontal planes. Applying the same method to cases for which $\Upsilon < 1$ would produce exactly the vertical sections visualised by Stevenson & Thomas [31] and Peat & Stevenson [34] for the uniform horizontal motion of oscillating cylinders and spheres.

Experiments of a different kind were achieved by Gilreath & Brandt [3] for internal waves generated by the turbulent wake of a slender spheroid, at large distances from the wake and under conditions for which $\Upsilon = 50$. From measurements of the displacement field on a vertical array of probes, and extraction of the random component by ensemble averaging over a large number of realisations of the same experiment, Gilreath & Brandt have shown that, in the plane $y = 0$, random internal waves are confined within a wedge of apex at the source and axis the x_1 -axis. Equation (4.6) gives for this wedge the semi-angle

$$\theta_c = \frac{2}{3^{\frac{3}{2}} \Upsilon} \approx \frac{0.385}{\Upsilon}, \quad (4.10)$$

which is precisely the theoretical law mentioned without proof and successfully compared with experiment by Gilreath & Brandt, and is also akin to the law obtained by Bonneton *et al.* [5] through a totally different reasoning.

Most of the ideas exposed in this paper arose from discussions with Drs Jean-Marc Chomaz, Philippe Bonneton, and Professor Emil J. Hopfinger. This work was supported by the Direction de la Recherche et des Etudes Techniques under Contract n°90/233.

References

- [1] E. J. HOPFINGER, Turbulence in stratified fluids: a review. *J. Geophys. Res.* **92**, 5287–5303 (1987).
- [2] J.-T. LIN & Y.-H. PAO, Wakes in stratified fluids. *Ann. Rev. Fluid Mech.* **11**, 317–338 (1979).
- [3] H. E. GILREATH & A. BRANDT, Experiments on the generation of internal waves in a stratified fluid. *AIAA J.* **23**, 693–700 (1985).
- [4] E. J. HOPFINGER, J.-B. FLOR, J.-M. CHOMAZ & P. BONNETON, Internal waves generated by a moving sphere and its wake in a stratified fluid. *Exp. Fluids* **11**, 255–261 (1991).
- [5] P. BONNETON, J.-M. CHOMAZ & E. J. HOPFINGER, Internal waves produced by the turbulent wake of a sphere moving horizontally in a stratified fluid. Submitted to *J. Fluid Mech.* (1992).
- [6] B. VOISIN, Rayonnement des ondes internes de gravité. Applications aux corps en mouvement. Ph.D. thesis, Université Pierre et Marie Curie (1991).
- [7] J. W. MILES, Internal waves generated by a horizontally moving source. *Geophys. Fluid Dyn.* **2**, 63–87 (1971).
- [8] S. A. MAKAROV & YU. D. CHASHECHKIN, Apparent internal waves in a fluid with exponential density distribution. *J. Appl. Mech. Tech. Phys.* **22**, 772–779 (1981).
- [9] G. S. JANOWITZ, Lee waves in three-dimensional stratified flow. *J. Fluid Mech.* **148**, 97–108 (1984).
- [10] M. UMEKI & T. KAMBE, Stream patterns of an isothermal atmosphere over an isolated mountain. *Fluid Dyn. Res.* **5**, 91–109 (1989).
- [11] R. J. HARTMAN & H. W. LEWIS, Wake collapse in a stratified fluid: linear treatment. *J. Fluid Mech.* **51**, 613–618 (1972).
- [12] J. C. S. MENG & J. W. ROTTMAN, Linear internal waves generated by density and velocity perturbations in a linearly stratified fluid. *J. Fluid Mech.* **186**, 419–444 (1988).
- [13] V. A. GORODTSOV, Evolution of axisymmetric vorticity distributions in an ideal incompressible stratified liquid. *Appl. Maths Mech.* **47**, 479–484 (1983).
- [14] V. A. GORODTSOV, Collapse of asymmetric perturbations in a stratified fluid. *Fluid Dyn.* **26**, 834–840 (1991).
- [15] P. BONNETON & J.-M. CHOMAZ, Instabilités du sillage généré par une sphère. *C. R. Acad. Sci. Paris II* **314**, 1001–1006 (1992).
- [16] J.-M. CHOMAZ, P. BONNETON & E. J. HOPFINGER, The structure of the near wake of a sphere moving horizontally in a stratified fluid. Submitted to *J. Fluid Mech.* (1992).
- [17] E. YA. SYSOEVA & YU. D. CHASHECHKIN, Vortex structure of a wake behind a sphere in a stratified fluid. *J. Appl. Mech. Tech. Phys.* **27**, 190–196 (1986).
- [18] E. YA. SYSOEVA & YU. D. CHASHECHKIN, Vortex systems in the stratified wake of a sphere. *Fluid Dyn.* **26**, 544–551 (1991).
- [19] D. L. BOYER, P. A. DAVIES, H. J. S. FERNANDO & X. ZHANG, Linearly stratified flow past a horizontal circular cylinder. *Phil. Trans. R. Soc. London A* **328**, 501–528 (1989).
- [20] Q. LIN, D. L. BOYER & H. J. S. FERNANDO, Turbulent wakes of linearly stratified flow past a sphere. *Phys. Fluids A* **4**, 1687–1696 (1992).
- [21] J. M. CIMBALA & W. J. PARK, An experimental investigation of the turbulent structure in a two-dimensional momentumless wake. *J. Fluid Mech.* **213**, 479–509 (1990).
- [22] H. HIGUCHI & T. KUBOTA, Axisymmetric wakes behind a slender body including zero-momentum configurations. *Phys. Fluids A* **2**, 1615–1623 (1990).
- [23] J. WU, Mixed region collapse with internal wave generation in a density-stratified medium. *J. Fluid Mech.* **35**, 531–544 (1969).
- [24] P. M. MORSE & H. FESHBACH, *Methods of Theoretical Physics. Part I.* MacGraw-Hill (1953).
- [25] B. VOISIN, Internal wave generation in uniformly stratified fluids. Part 1. Green’s function and point sources. *J. Fluid Mech.* **231**, 439–480 (1991).
- [26] R. E. DICKINSON, Propagators of atmospheric motions. 1. Excitation by point impulses. *Rev. Geophys.* **7**, 483–514 (1969).
- [27] S. YA. SEKERZH-ZEN’KOVICH, A fundamental solution of the internal-wave operator. *Sov. Phys. Dokl.* **24**, 347–349 (1979).
- [28] N. A. ZAVOL’SIIH & A. A. ZAITSEV, Development of internal waves generated by a concentrated pulse source in an infinite uniformly stratified fluid. *J. Appl. Mech. Tech. Phys.* **25**, 862–867 (1984).

- [29] T. N. STEVENSON, The phase configuration of internal waves around a body moving in a density stratified fluid. *J. Fluid Mech.* **60**, 759–767 (1973).
- [30] T. I. MCLAREN, A. D. PIERCE, T. FOHL & B. L. MURPHY, An investigation of internal gravity waves generated by a buoyantly rising fluid in a stratified medium. *J. Fluid Mech.* **57**, 229–240 (1973).
- [31] T. N. STEVENSON & N. H. THOMAS, Two-dimensional internal waves generated by a travelling oscillating cylinder. *J. Fluid Mech.* **36**, 505–511 (1969).
- [32] L. G. REDEKOPP, Wave patterns generated by disturbances travelling horizontally in rotating stratified fluids. *Geophys. Fluid Dyn.* **6**, 289–313 (1975).
- [33] R. G. REHM & H. S. RADT, Internal waves generated by a translating oscillating body. *J. Fluid Mech.* **68**, 235–258 (1975).
- [34] K. S. PEAT & T. N. STEVENSON, Internal waves around a body moving in a compressible density-stratified fluid. *J. Fluid Mech.* **70**, 673–688 (1975).
- [35] B. VOISIN, Internal wave generation in uniformly stratified fluids. Part 2. Moving point sources. Submitted to *J. Fluid Mech.* (1992).

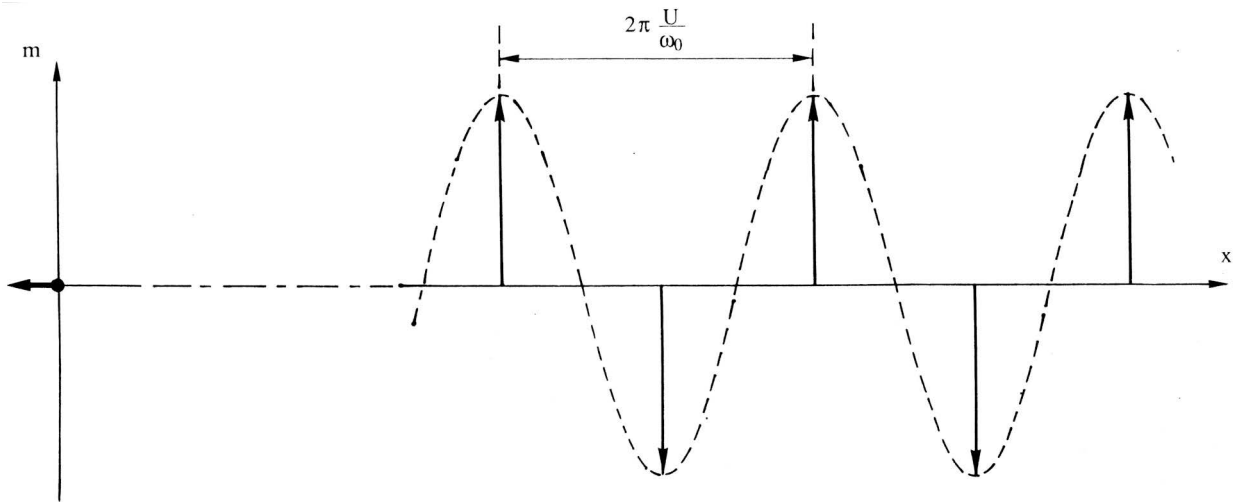


FIGURE 1. Turbulent wake model; (—) impulsive model (2.1), (---) oscillating model (4.1).

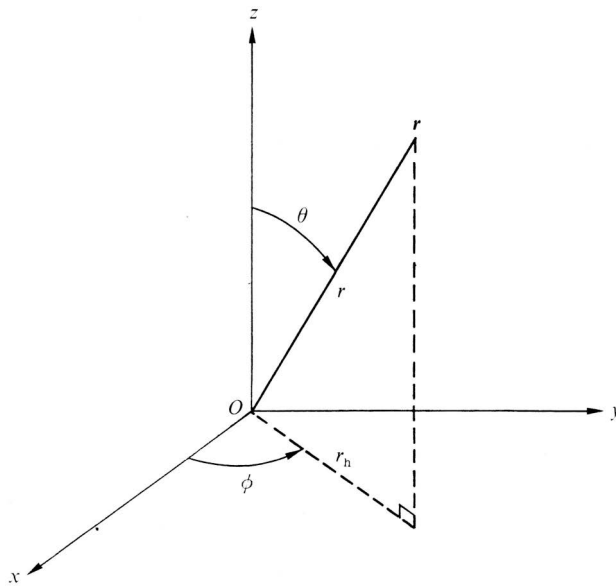


FIGURE 2. System of coordinates for wave generation by the isolated collapse (3.1) (from [25]).

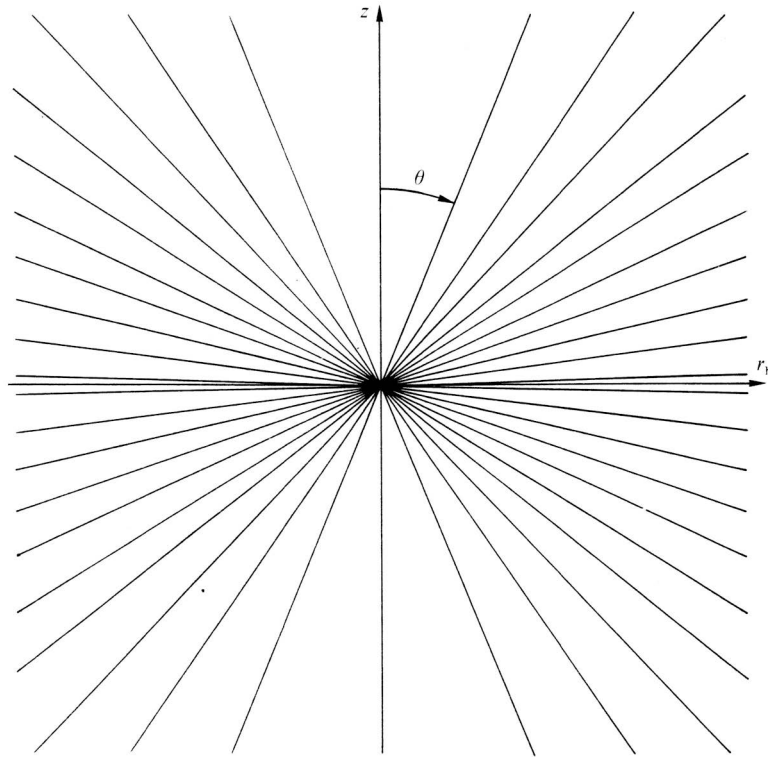


FIGURE 3. Surfaces of constant phase $\Phi = \pi/4 + n\pi$ for a point impulsive source, for $Nt = 10\pi$ (from [25]).

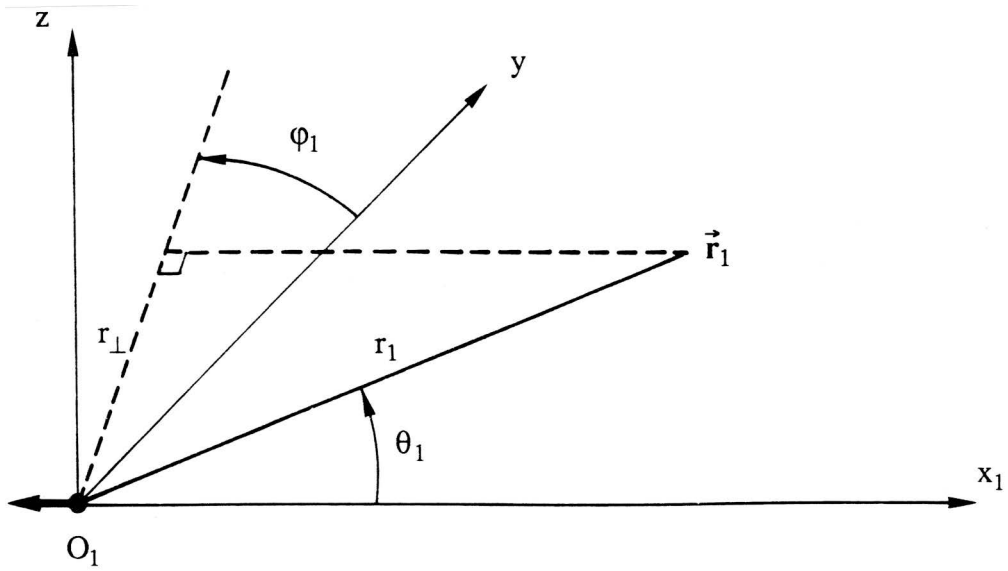


FIGURE 4. System of coordinates for wave generation by the collection of collapses (4.1) (from [35]).

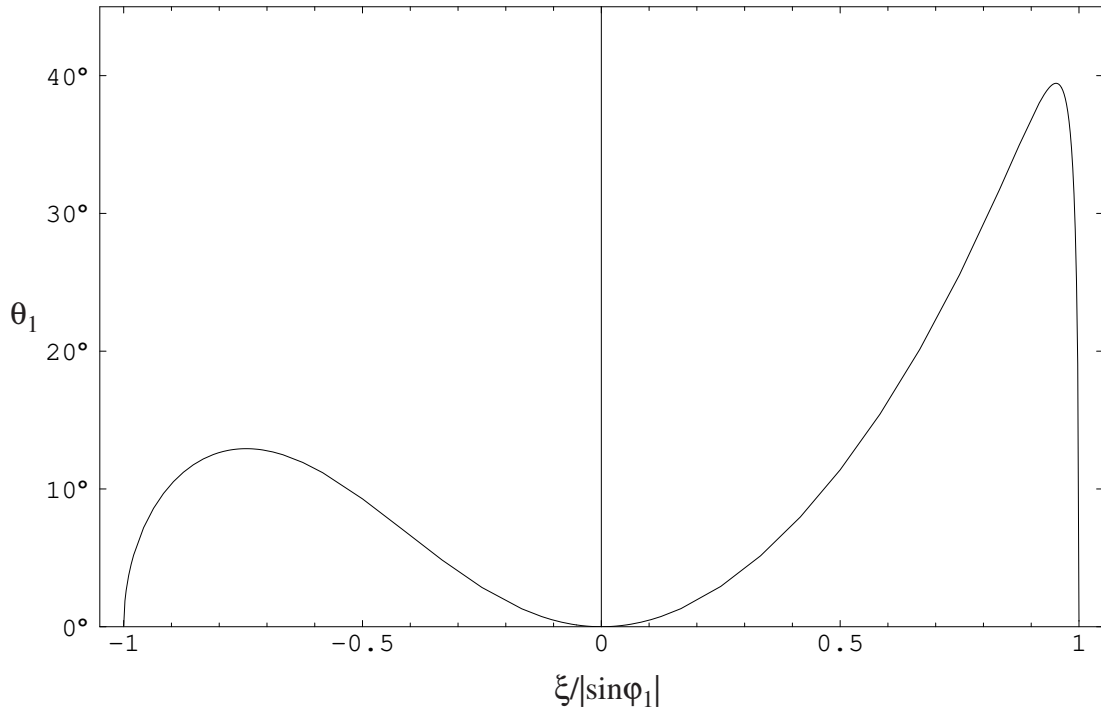


FIGURE 5. Graphical solution of equation (4.4) for the reduced frequency ξ , for $\Upsilon/|\sin \varphi_1| = 1.2$ (from [35]).

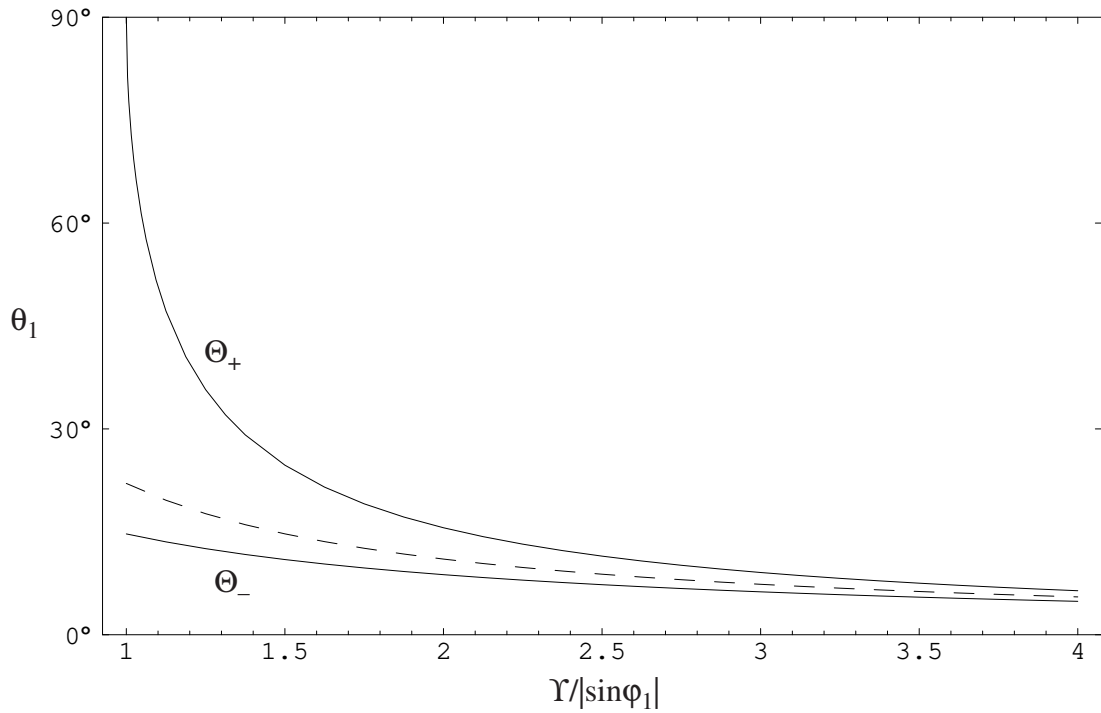
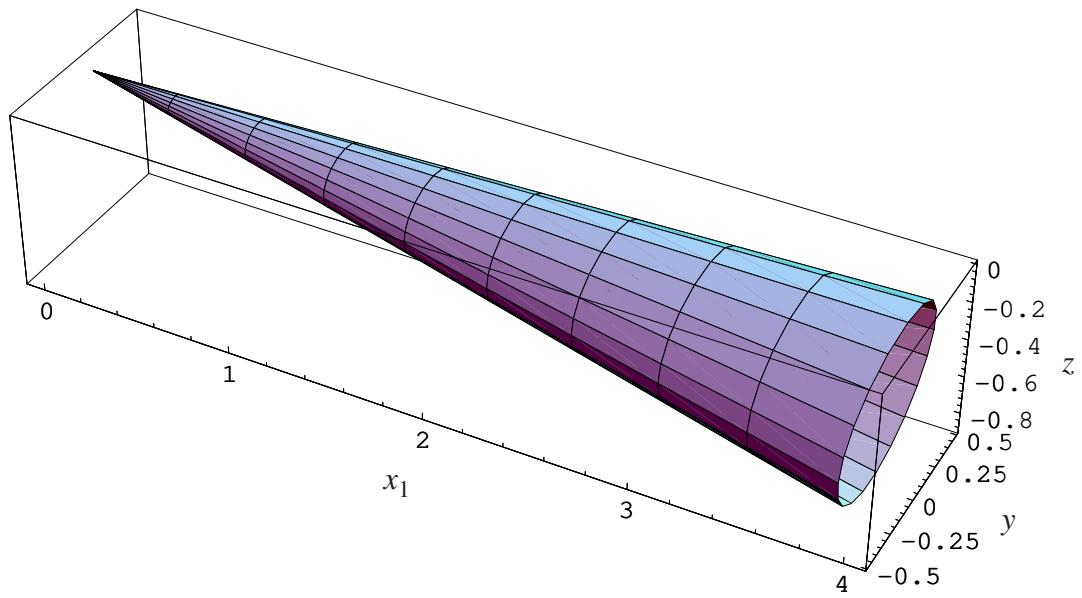
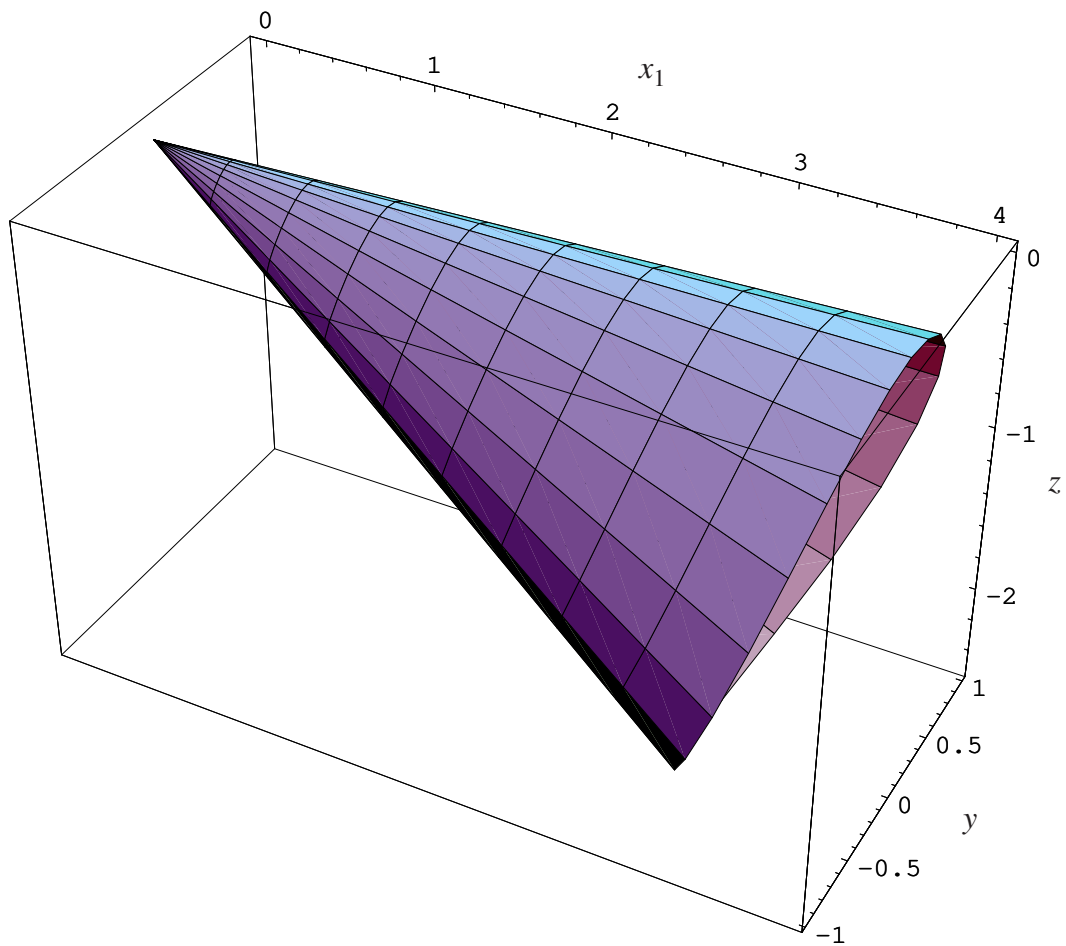


FIGURE 6. Equation of the caustics for an oscillating source in uniform horizontal motion; (—) exact equation (4.5), (---) asymptotic equation (4.6) (from [35]).

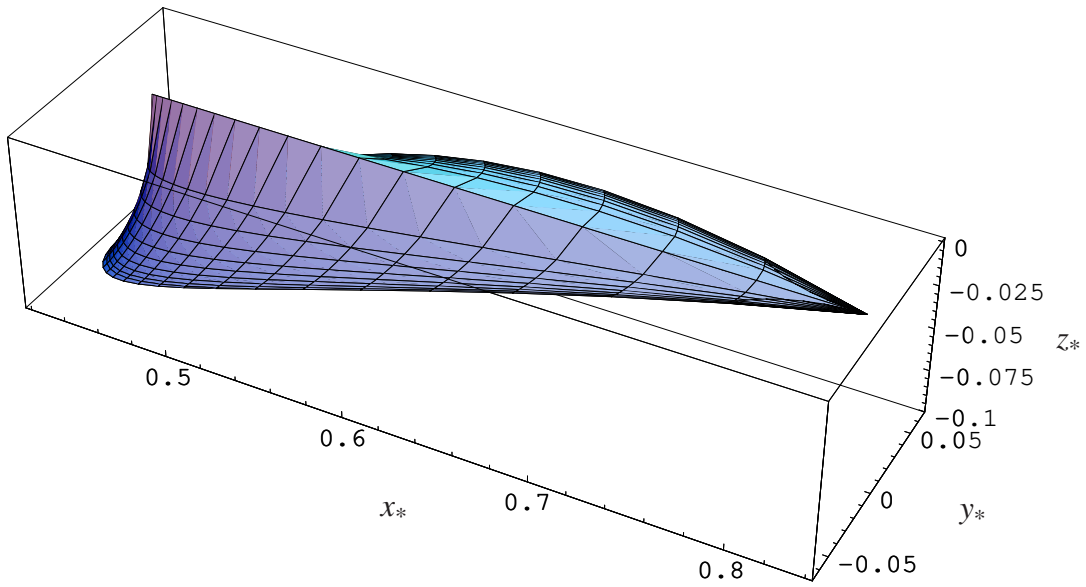


(a)

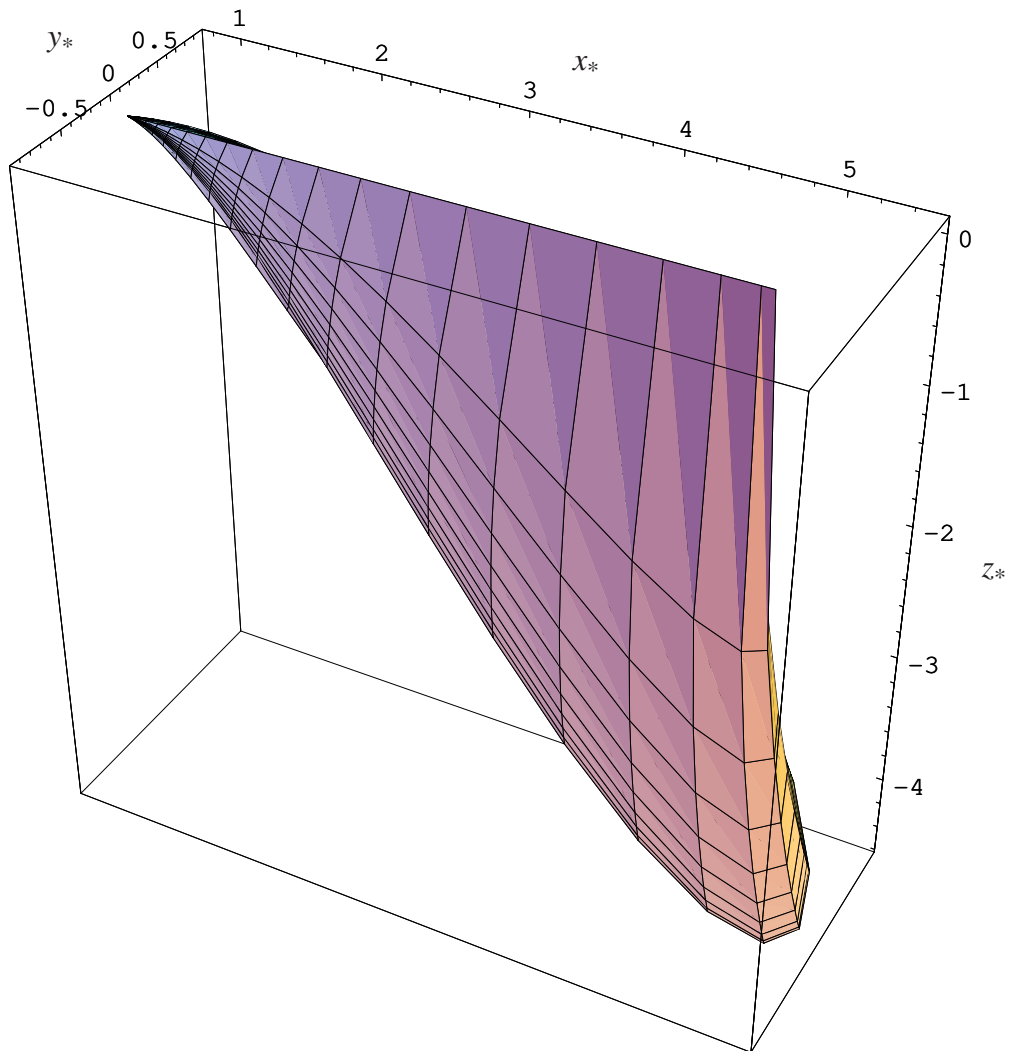


(b)

FIGURE 7. Caustics for an oscillating source in uniform horizontal motion, for $\Upsilon = 1.2$; (a) difference waves, (b) sum waves. Only the lower half of the caustics, symmetric with respect to the plane $z = 0$, is shown (from [35]).



(a)



(b)

FIGURE 8. Perspective view of surfaces of constant phase for an oscillating source in uniform horizontal motion, for $\mathcal{T} = 1.2$; (a) difference waves, (b) sum waves. Only the lower half of those surfaces, symmetric with respect to the plane $z = 0$, is shown (from [35]).

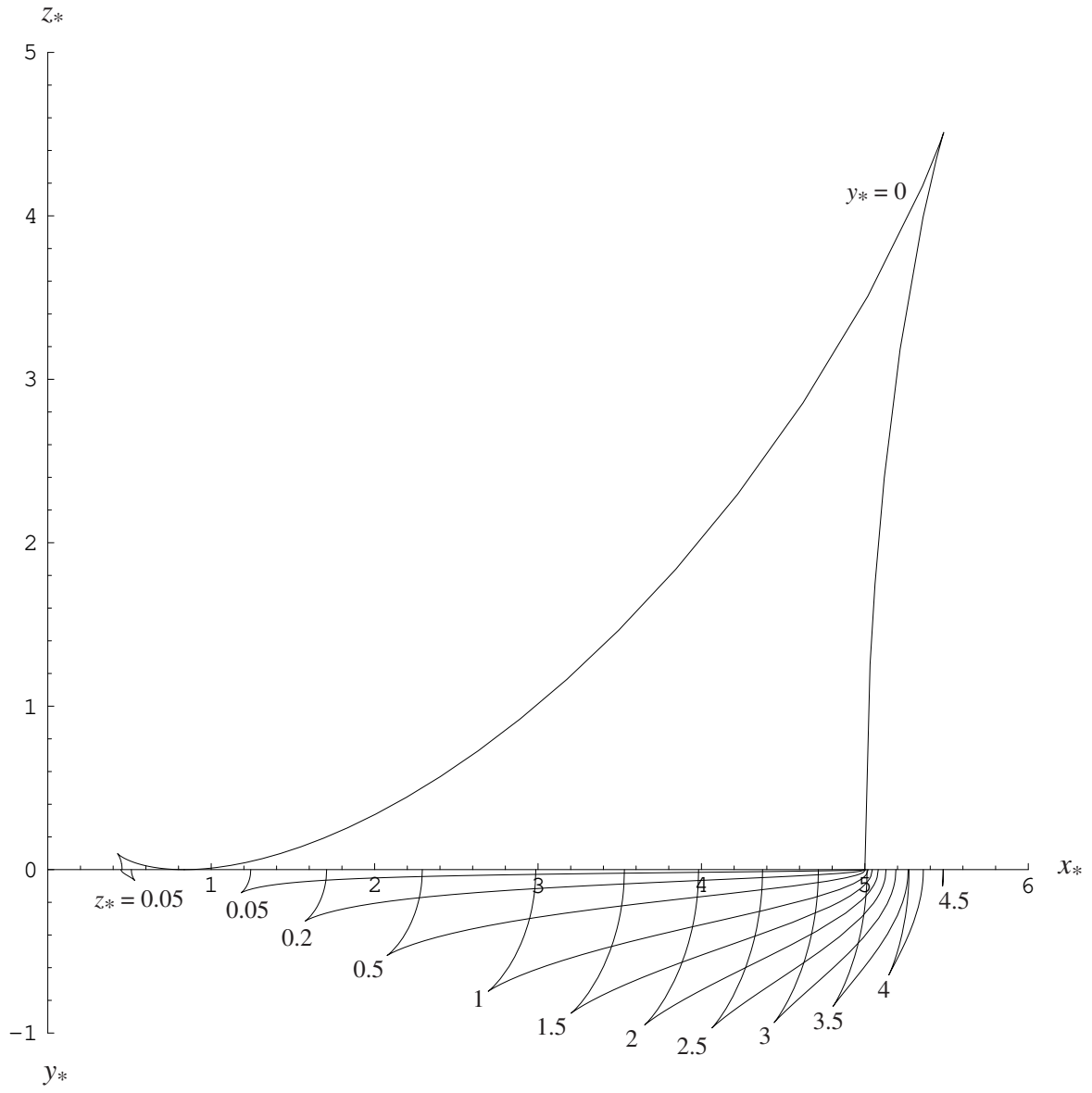


FIGURE 9. Two-dimensional view of surfaces of constant phase for an oscillating source in uniform horizontal motion, for $\mathcal{T} = 1.2$ (from [35]).